Caving 2022 - Y Potvin (ed.)

doi:10.36487/ACG_repo/2205_10

Large-scale dynamic testing of ground support systems at the Walenstadt testing facility

R Brändle *Geobrugg, Switzerland*

R Luis Fonseca *Geobrugg, Switzerland*

G von Rickenbach *Geobrugg, Switzerland*

G Fischer *Geobrugg, Switzerland*

JA Vallejos *Advanced Mining Technology Center, Universidad de Chile, Chile*

E Marambio *Advanced Mining Technology Center, Universidad de Chile, Chile*

L Burgos *Advanced Mining Technology Center, Universidad de Chile, Chile*

D Cuello *Advanced Mining Technology Center, Universidad de Chile, Chile*

Abstract

Ground support systems must provide safe and effective designs for underground excavations under high stress conditions. These systems must be capable to resist dynamic impacts and yielding during the loading process. In this context dynamic testing of the reinforcement and retaining elements that compose the ground support system are required to study and improve the behaviour of these elements under dynamic load events. During the last years, Geobrugg has been working on the improvement of retaining products by testing them in a large-scale impact test facility located at Walenstadt, Switzerland. The test facility is composed of a double level platform with a square-shaped pyramidal trunk geometry, the upper level houses a loading mass that drops from a height up to 5 m. The loading mass is guided by one central steel pipe, and the impact occurs in the sample to be tested, which is located at the lower level in a slab with an area of 3.6 m × 3.6 m. This is where the ground support system is installed. During the last few years, this innovative facility has been used to test several configurations of ground support systems. The results of these tests have enabled the authors to improve the understating of the behaviour of ground support systems under dynamic loads. In this manuscript, the arrangement, measurement, results, and the preliminary analysis of large-scale dynamic tests of two ground support systems performed in 2019 and 2021, supported by the Advanced Mining Technology Center (AMTC – University of Chile), are presented.

Keywords: *ground support, high stress conditions, rockburst, dynamic testing, underground excavations*

1 Introduction

Mining conditions are becoming increasingly difficult because ore deposits are getting deeper, the high stress environments cause many challenges to continue exploiting resources. One of the main issues is related to the occurrence of seismic events and the associated rockburst phenomenon, which leads to operational and safety problems.

The amount of energy release during seismic events requires mitigation by ground support systems (reinforcement plus retainment systems) that are able to control large displacements and high strain rates. These dynamic systems are composed of reinforcement elements (e.g. rockbolts, cable bolts) able to absorb a large amount of energy and surface support (e.g. meshes) that provide containment to the rock mass (Zhou & Zhao 2011).

The design of ground support systems requires research into the behaviour of each support element under dynamic loading. Previously, several tests have been carried out on individual bolts, cables, and meshes, but

in practice, all components must fit and work together. Thus, the testing is relevant to assess and increase, if necessary, the performance of support elements and offer industry these improved designs. Some institutions in Canada, South Africa and Australia have been testing reinforcement and support elements under dynamic loads. However, the facilities that can test the combinations (reinforcement or ground support systems) of rockbolts, cable bolts, and mesh as a system are limited.

Over the years, large-scale tests have been conducted in the rockfall testing facility at Walenstadt, Switzerland, that have contributed to improving knowledge and the trial of different types of test configurations and sample configurations (Brändle et al. 2021, 2020, 2017; Brändle & Luis Fonseca 2019; Bucher et al. 2013; Cala et al. 2013; Muñoz et al. 2017; Roth et al. 2014). In this context, since 2018 Geobrugg and the Advanced Mining Technology Center (AMTC – University of Chile) have been collaborating to improve the performance of ground support systems under dynamic loads (rockburst prone) considering large-scale tests, back-analysis, numerical modelling, and design. Therefore, this paper presents the testing arrangement, measurement, results, and the preliminary analysis of large-scale dynamic test of two ground support systems performed in 2019 and 2021.

2 Dynamic laboratory tests

During the last 30 years, significant effort has been made to obtain and quantify the dynamic response of a complete ground support system to provide solutions for rockburst control in high stress mining environments. Testing and the measurements of dynamic responses of isolated components that comprise the ground support system, such as rockbolts, cable bolts or meshes, have been conducted by a number of institutions, including CanMet-MMSL, Western Australia School of Mines (WASM) and New Concept Mining (Crompton et al. 2018; Kaiser et al. 1996; Player et al. 2004). In addition, simplified retention (load distribution) and ground support systems have been tested by projects such as Safety in Mines Research Advisory Committee (SIMRAC)/SRK or Geomechanics Research Centre (GRC) (Cai & Kaiser 2018; Kaiser et al. 1996; Ortlepp 2001; Ortlepp & Stacey, 1998, 1997) using the impact principle and the momentum transfer concept (WASM). Figure 1 illustrates the dynamic facilities of CanMet-MMSL, WASM and New Concept Mining, respectively. Whereas Figure 2 shows the SIMRAC/SRK apparatus and the GRC apparatus, respectively. Table 1 illustrates a summary of the facilities able to test configurations of ground support or retention (load distribution) systems.

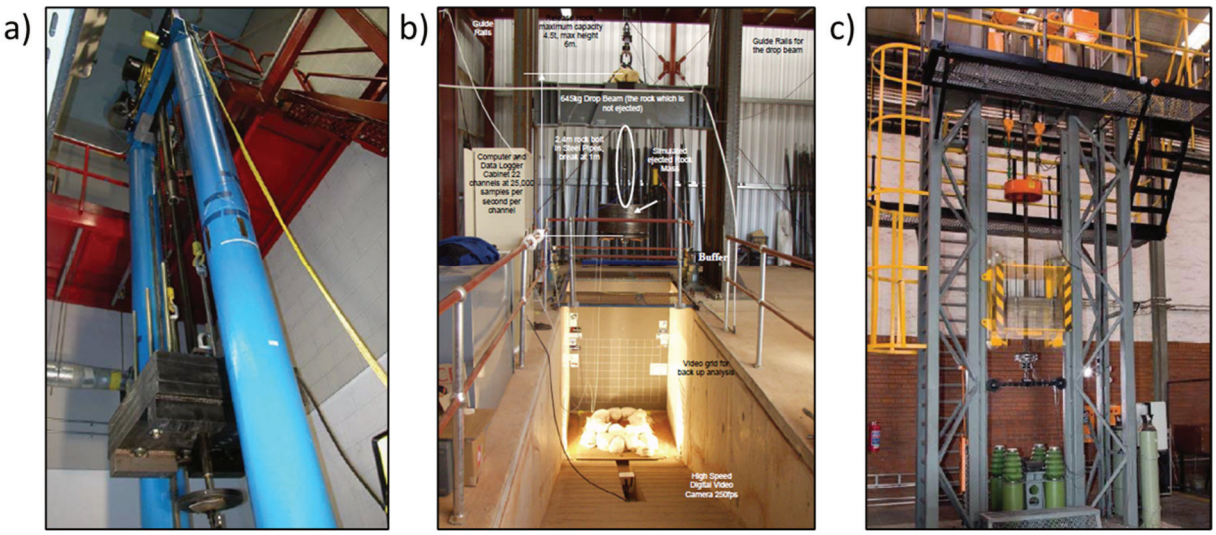

Figure 1 (a) CanMet-MMSL facility (Cai & Kaiser 2018); (b) WASM facility (Player et al. 2004); (c) New Concept Mining facility (Crompton et al. 2018)

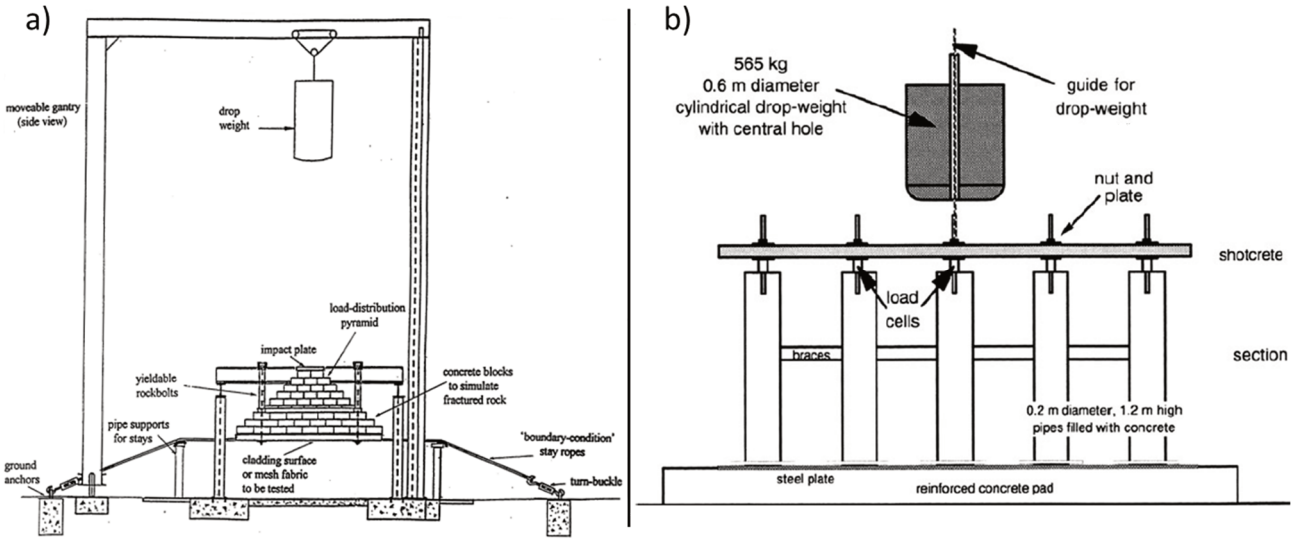

Figure 2 **(a) SIMRAC/SRK apparatus (Ortlepp & Stacey 1997); (b) GRC apparatus (Kaiser et al. 1996)**

Table 1 **Summary of the facilities that test ground support or retainment systems (modified from Hadjigeorgiou & Potvin 2011)**

Facility	Configuration/ element tested	Loading mass (kg)	Drop height (m)	Impact velocity (m/s)	Impact energy (kJ)	Test area	Measurement instruments
WASM Dynamic facility	Reinforcement elements and surface support	Up to 4,500	Up to 6	Up to 10	Up to 225	1 × 1 m	High-speed cameras, photographs, load cells, accelerometers and reference tapes
SRK Drop weight test	Support system	Up to 2,700	3.3	8.1	Up to 80	2 × 2 m	High-speed cameras, photographs and reference tapes
SIMRAC Dynamic testing rig	Support system	1,000					Telescopic bars and geophones
SIMRAC Dynamic stope test	Stope support system	10,000	3	7.7	Up to 294	3 × 3 m	High-speed cameras, photographs and reference tapes
GRC Support element test	Reinforced shotcrete	565	4	8.8	22		Load cells and photographs
Geobrugg Walenstandt test	Support system	Up to 9,640	5	10	Up to 500	3.6 × 3.6 m	High-speed cameras, photographs, accelerometers, load cells and reference tapes

The dynamic testing of the retaining and ground support systems has been limited due to the difficulty in representing the in situ conditions of a seismic event, quantifying the damage, measuring, and validating the response of each element and the interaction among them. Geobrugg has been performing real scale dynamic tests on ground retainment and ground support systems using the impact principle (drop weight test) since the research programme started by Cala et al. (2013) at the facility in Walenstadt, Switzerland. The Walenstadt facility has been improved over the years in order to better represent and understand the damage process that occurs to a complete ground support system during a dynamic impact that represents the in situ conditions of a seismic event (Brändle et al. 2021, 2020, 2017; Brändle & Luis Fonseca 2019; Bucher et al. 2013; Cala et al. 2013; Muñoz et al. 2017; Roth et al. 2014).

Figures 3a and 3b show a schematic of the dynamic testing facility at Walenstadt used in the double impact test (test performed in 20219), whereas Figure 3c illustrates the current facility in situ.

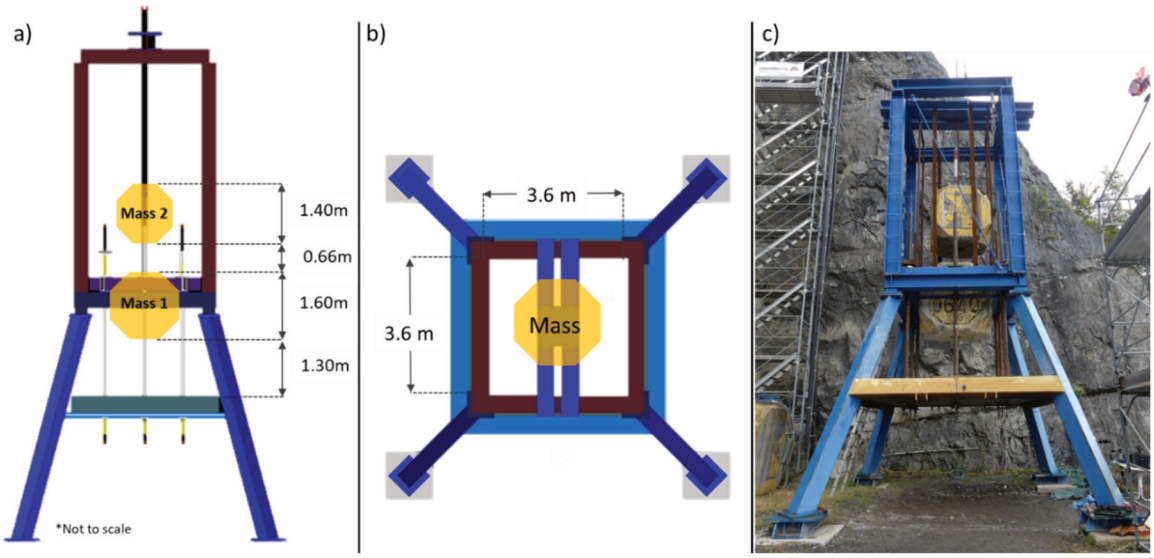

Figure 3 (a) Front view of testing setup; (b) Plan view of testing setup; (c) Dynamic test facility at Walenstadt (test performed in 2019)

2.1 Test arrangement

The testing setup to perform and record the dynamic tests comprises the following components.

For the test performed in 2019:

- Steel pipes of 10 mm thickness with an inner diameter of 45 mm that represent the boreholes in which the rockbolts are installed in situ. In this test nine steel pipes were used (for different rockbolt patterns), and the central steel pipe also served as a guide for the loading masses.
- A lower loading mass (mass 1 in Figure 3a) of 9,640 kg released in a free fall condition along the central steel pipe from a height of 1.30 m.
- An upper loading mass (mass 2 in Figure 3a) of 6,400 kg released in a free fall condition along the central steel pipe from a height of 1.96 m. This second mass was attached to the first mass with cables and was released together. Both masses lead to a nominal input energy of 245 kJ.

For the test performed in 2021:

- As with the previous test, in this test nine steel pipes were used, and the central steel pipe also served as a guide for the loading mass.
- One loading mass of 9,640 kg released in a free fall condition along the central steel pipe from a height of 2.5 m (as reference, the same mass 1 in Figure 3a). This leads to a nominal input energy of 235 kJ.

In these arrangements no distribution elements were used to transmit the input energy to the load distribution systems tested. In addition, the use of these masses (two and one, respectively) in the dynamic tests represent the dynamic loading condition of two typical seismic events where these ground support systems are commonly implemented. In this sense, the length of the cables that join both masses in the test performed in 2019 represent the time gap between the two impacts proportional to the in situ seismic event recorded at that time.

2.2 Ground support system

Both test setups were built based on two similar ground support systems used at CODELCO – El Teniente Mine, which includes the following.

For the test performed in 2019:

- A retainment (load distribution) system with a test area of 3.6 m × 3.6 m composed by the first layer of shotcrete with a thickness of 5 cm; then Geobrugg's chain link mesh (internal) made of high-tensile steel wire with a diameter of 4 mm (MINAX 80/4); the second layer of shotcrete with a thickness of 2 cm; and a second Geobrugg's MINAX 80/4 mesh (external). Figure 4a illustrates a scheme of the MINAX 80/4 high-tensile mesh and Figure 4b shows the properties of the MINAX 80/4 high-tensile mesh.
- A reinforcement system composed by nine threadbars (rockbolts) with a diameter of 25 mm, a length of 4 m and made of A630 Chilean steel grade. The rockbolts were located in a square pattern of 1 m × 1 m and embedded into the steel pipes with cement grout. After curing, each rockbolt was attached to the retainment system using a double plate and double nut (one pair per mesh). In this case, each rockbolt was debonded by sheathing covering a length of 50 cm from the collar (retainment system) to represent the fractured rock zone in situ. Figures 5a and 5b illustrate the test configuration with each rockbolt identified (ID number) from an upper and lower view of the ground support system, respectively.

For the test performed in 2021:

- A load distribution system with a test area of 3.6 m × 3.6 m composed by a layer of shotcrete with a thickness of 7 cm; and a Geobrugg's chain link mesh (external) made of high-tensile steel wire with a diameter of 4.6 mm (MINAX 80/4.6). Figure 4a also illustrates the scheme of the MINAX 80/4.6 high-tensile mesh and Figure 4b also shows the properties of the MINAX 80/4.6 high-tensile mesh.
- The reinforcement system in this case was similar to the previous test. However, after curing each rockbolt, the reinforcement system was attached to the load distribution system using the typical plate and nut. In this case, each rockbolt was also debonded by sheathing covering a length of 50 cm from the collar (load distribution system) to represent the fractured rock zone in situ. Figure 5c and 5d illustrate the test configuration with each rockbolt identified (ID number) from an upper and lower view of the ground support system, respectively.

It is of note that both load distribution systems were built before testing, with enough time to cure the shotcrete at least 28 days and were subsequently attached to the reinforcement systems on the frame. Figure 6 shows a cross-section scheme of each ground support systems tested.

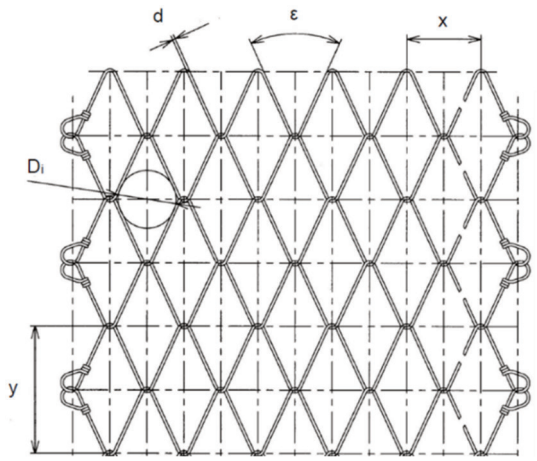

Properties	MINAX 80/4	MINAX 80/4.6
Mesh width (D_i)	80 (mm)	80 (mm)
Diagonal ($x \cdot y$)	102 × 177 (mm)	100 × 174 (mm)
Wire diameter (d)	4 (mm)	4.6 (mm)
Wire strength (f_i)	1,770 (MPa)	>1,770 (MPa)
Tensile resistance of a wire (z_w)	22 (kN)	29.4 (kN)
Tensile strength of mesh longitudinal (z_l)	190 (kN/m)	285 (kN/m)
Weight per m²	2.6 (kg/m²)	3.4 (kg/m²)

(a) (b)

Figure 4 Diamond-shaped high-tensile mesh (MINAX 80/4 and MINAX 80/4.6 of Geobrugg). (a) Plan view scheme; (b) Properties of both meshes

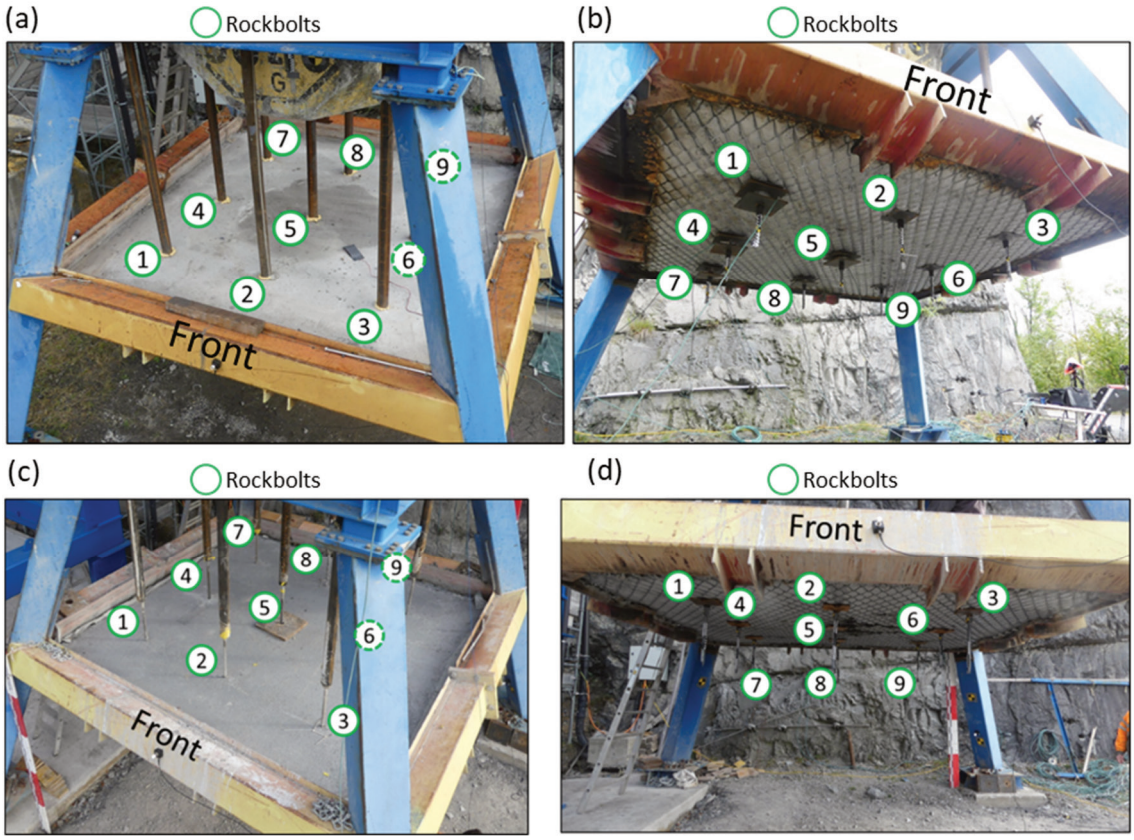

Figure 5 Test performed in 2019: (a) Upper view; (b) lower view of the test configuration with each rockbolt identified (ID number). Test performed in 2021: (c) Upper view; (d) Lower view of the test configuration with each rockbolt identified (ID number)

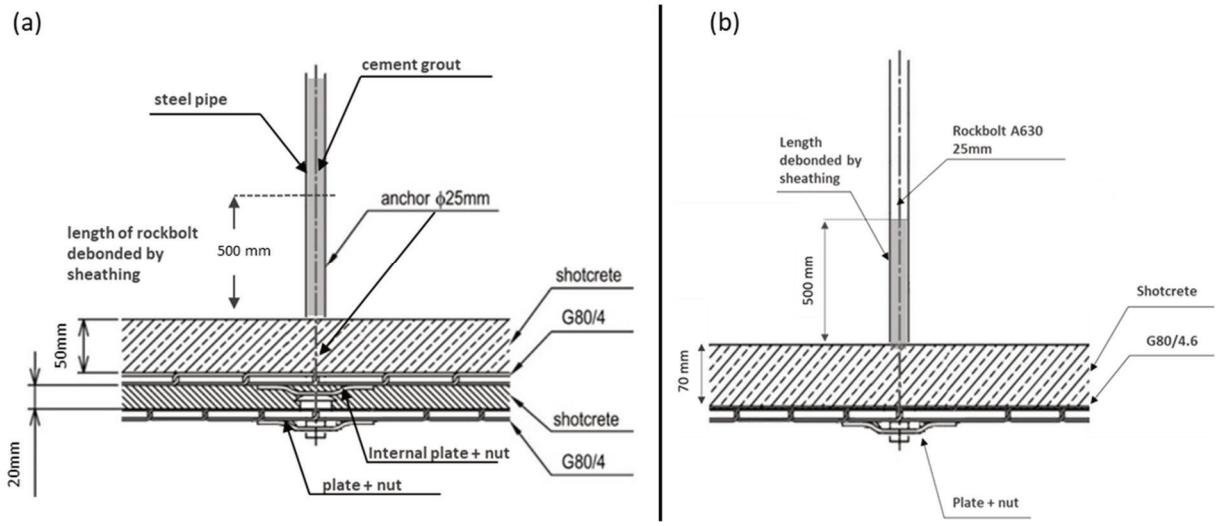

Figure 6 Cross-section of the ground support systems tested: (a) Test performed in 2019; (b) Test performed in 2021

2.3 Measuring system

The measuring system used for both tests included:

- Four high-speed cameras: a first camera pointing to the upper area (internal face) of the retainment system, a second pointing to the lower area (external face) of the retainment system, a third camera pointing to the upper area (external face) of the retainment system located at 90 degrees from the first camera, and a fourth camera pointing to the lower area (external face) of the retainment system located at 90 degrees from the second camera. Figure 7a shows a high-speed camera used in both tests.
- One accelerometer was located at the lateral edge (or top) of each loading mass (in both tests). Figure 7b shows the accelerometers located at the upper and lower loading masses used in the test performed in 2019.
- For the test performed in 2019, ten load cells were used; five located at the collar (external plate) and five located at the anchor (upper part of the reinforcement system) of five rockbolts (i.e. rockbolts 1, 4, 5, 7 and 8 in Figure 5a and 5b), with the assumption of symmetrical response of the rockbolts due to the pattern of the reinforcement system. Figure 7c illustrates the load cells located at the collar of rockbolts 4, 7 and 8. Whereas Figure 7d illustrates the load cell located at the anchor of the rockbolt 7.
- For the test performed in 2021, four load cells were used (the same used in previous test). They were located at the anchor (upper part of the reinforcement system) of four rockbolts (i.e. rockbolts 5, 6, 8, and 9 in Figure 5a and 5b), with the assumption of symmetrical response of the rockbolts due to the pattern of the reinforcement system.
- Reference tapes located in each rockbolt and reference rulers to support the measurement of the high-speed cameras. Figure 7e shows an example of the reference tapes located in each rockbolt (each square represents an area of 1 cm^2), and a ruler located at the back of the apparatus for the test performed in 2021.
- A coordinate reference system for both tests located in the middle of the retainment system (origin) to support the measurement of the dynamic displacement as shown in Figure 7f. The positive axes point to the right (x), back (y) and upwards (z).

Table 2 illustrates the properties of the measuring instruments.

Figure 7 **(a) Front high-speed camera used in the tests; (b) Accelerometers located at the upper and lower loading mass (test 2019); (c) Load cells located at the collar of rockbolts number 4, 7 and 8 (test 2019); (d) Load cells located at the anchor of the rockbolts number 7 and 8 (test 2019); (e) Example of reference tapes located at rockbolts 8 and 9, and ruler located at the back of the apparatus (test 2021); (f) Coordinate system of the test field**

Table 2 **Properties of the measuring instruments**

Measuring Instrument	Properties
High-speed cameras	Recording frequency of 500 images per second
Accelerometers	2,000 g triaxial accelerometers with a frequency of 20 kHz
Load cells	750 kN force sensors with a frequency of 4.8 kHz
Reference tapes and rulers	Tapes with a square pattern of 1 cm^2 and rulers with a pattern of 10 cm

3 Test results

The behaviour of both ground support systems was recorded and analysed using the information collected by the measuring system. For the test performed in 2019, the impact loading masses were arrested to an equilibrium state by the ground support system with a final dynamic displacement of 0.29 m, and an impacted area located at the centre of the load distribution system as illustrated in Figure 8a. The impact of the loading masses caused the failure of rockbolt number 5 (central rockbolt) and some plates of other rockbolts caused a cut in the internal mesh.

In the case of the test performed in 2021, the impact loading mass was not arrested to an equilibrium state by the ground support system, leading to a failure of the entire support. The damaged area (crater) located at the centre of the load distribution system (final state) is illustrated in Figure 8b. The impact of the loading mass caused the failure of rockbolt 5 (central rockbolt) and some plates of other rockbolts caused a cut in the external mesh.

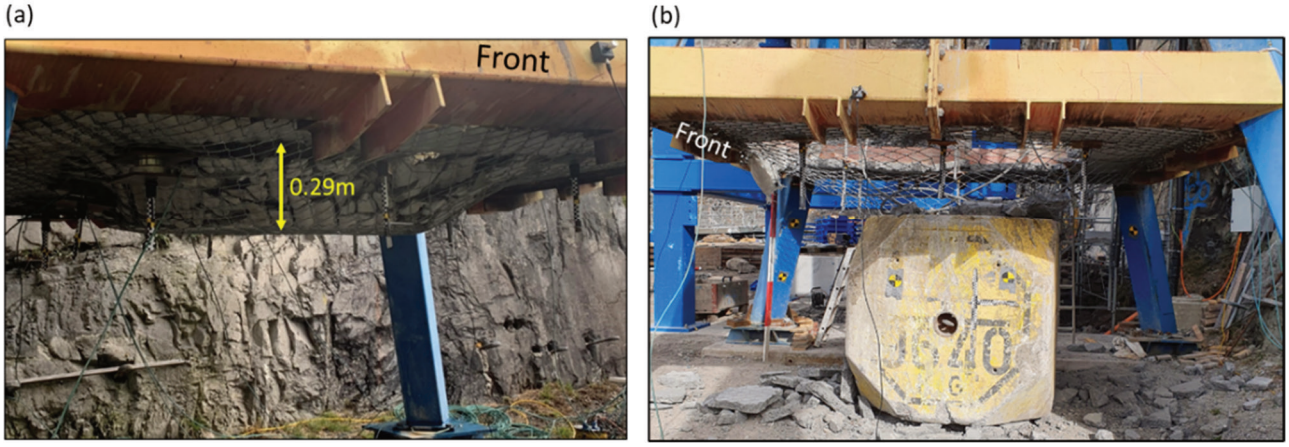

Figure 8 (a) Test 2019: Final dynamic displacement, and bagging area of the ground support system; (b) Test 2021: Final state of the ground support (damaged area)

Figure 9 illustrates the dynamic process recorded by the high-speed cameras at different instants of time for both tests. Whereas Figure 10a, 10b and 10c show the failure of rockbolt 5, and the cut in the internal mesh by the plate of rockbolt 2 after the test performed in 2019, respectively. In addition, Figure 10a shows the damaged area (crater) with some rockbolts detached after the test performed in 2021, and Figure 10b and 10c illustrate the deformation in rockbolt 4 after the same test.

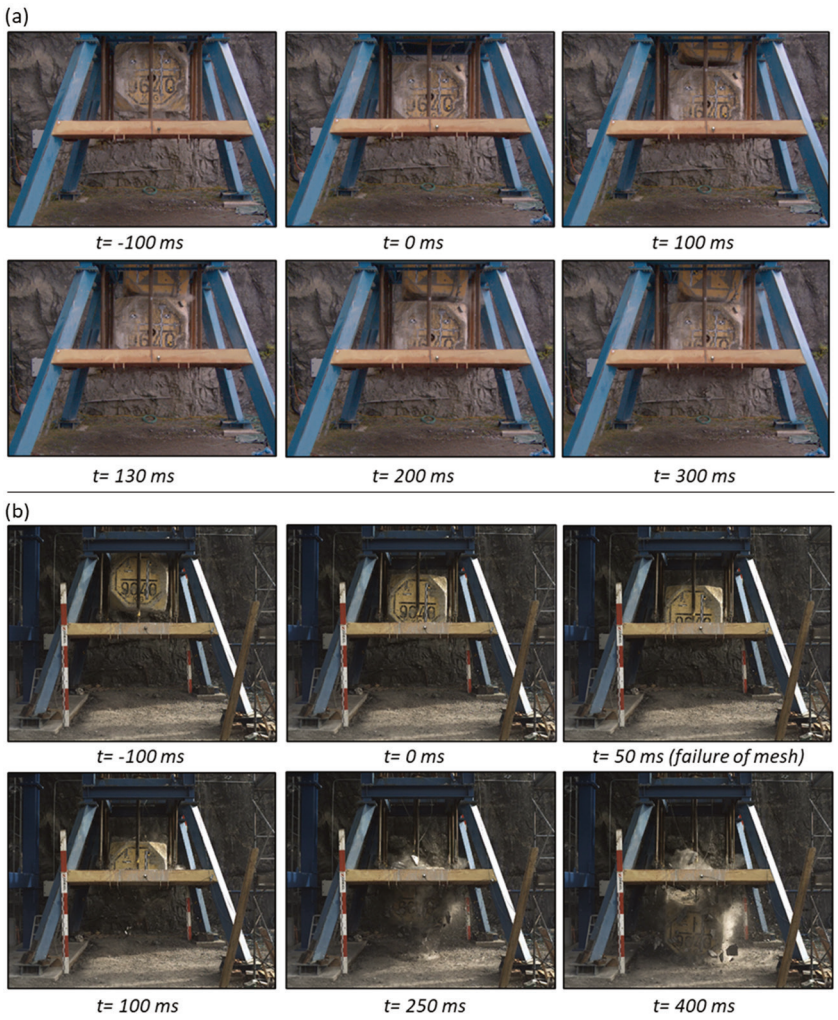

Figure 9 Dynamic loading process of both tests recorded by the high-speed cameras as a function of time. (a) Test performed in 2019; (b) Test performed in 2021

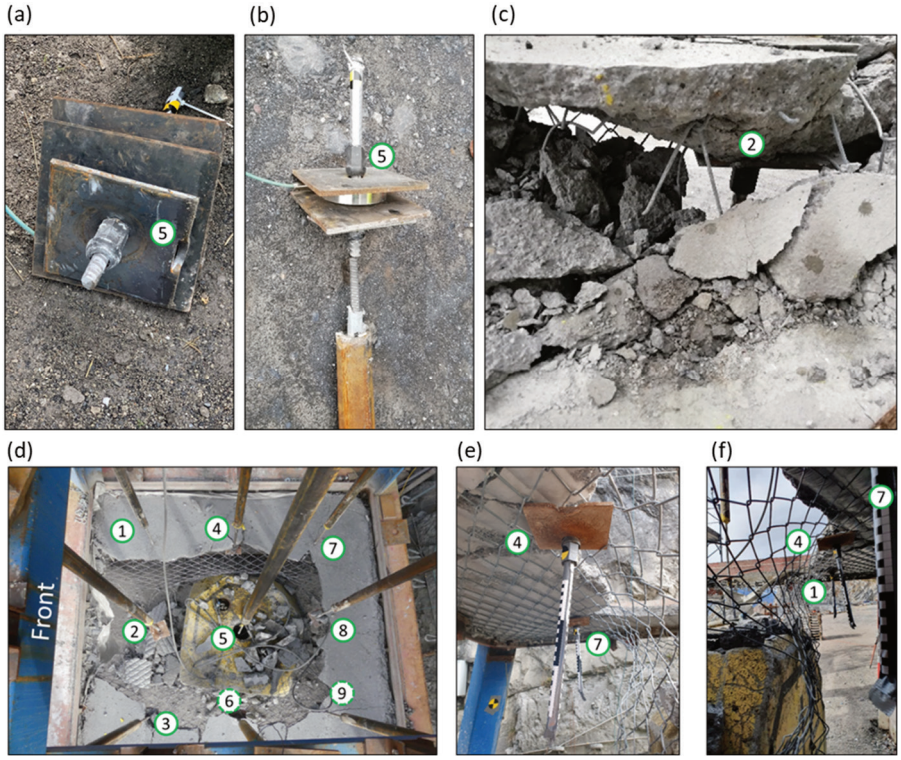

Figure 10 For the test performed in 2019: (a) Load cell, external plate and nut of rockbolt 5 after the test; (b) Failure of rockbolt 5 at the collar after the test; (c) Cut of the internal mesh by the plate at rockbolt 2. For the test performed in 2021: (d) Damaged area (crater) with some rockbolts detached after the test; (e) and (f) Detail of deformation in rockbolt 4 after the test

3.1 Analysis

As mentioned previously, the nominal input energy of the tests performed in 2019 and 2021 was 245 kJ and 235 kJ, respectively. However, after measuring the displacement of the ground support systems with the high-speed cameras and capturing the acceleration of the loading masses, the maximum measured input energy was 183 kJ and 120 kJ (at the point of failure), respectively (see Figure 13b).

Note that for the test performed in 2019, the second impact occurred at the time of 130 ms as shown in the acceleration record of Figure 11a. Whereas the failure of the ground support system tested in 2021 occurred at the time of 50 ms as shown in the acceleration and displacement record of Figure 11b.

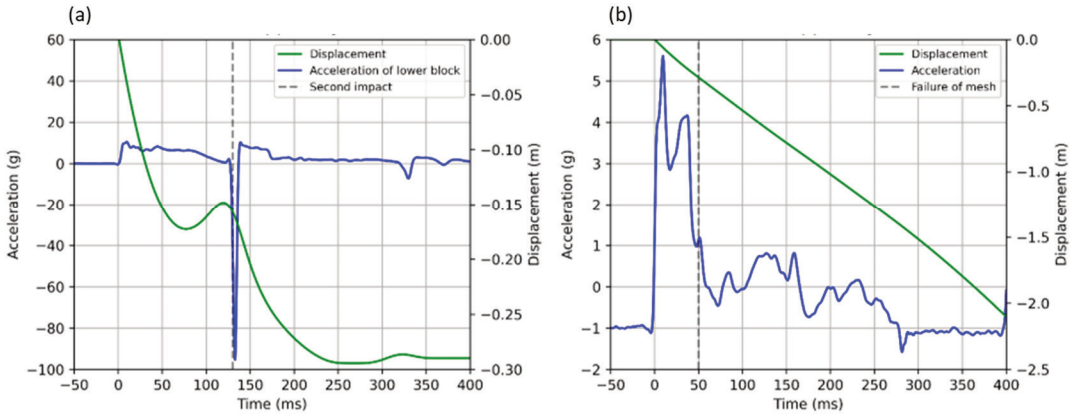

Figure 11 (a) Test 2019: Dynamic displacement and acceleration of the lower block as a function of time; (b) Test 2021: Dynamic displacement and acceleration of the loading mass (block) during the dynamic test

For the test performed in 2019, the load capacity of the rockbolts during the impact of the two masses was recorded by the load cells. The records of the load cells located at the anchor (upper) and collar (lower) of the rockbolts are shown in Figure 12a.

In the case of the test performed in 2021, the records of the load cells located at the anchor (upper part) of the rockbolts are shown in Figure 12b. Note that the failure of rockbolt 5 (central rockbolt) occurred at the time of 40 ms.

The maximum measured capacities of the rockbolts in both tests are illustrated in Table 3.

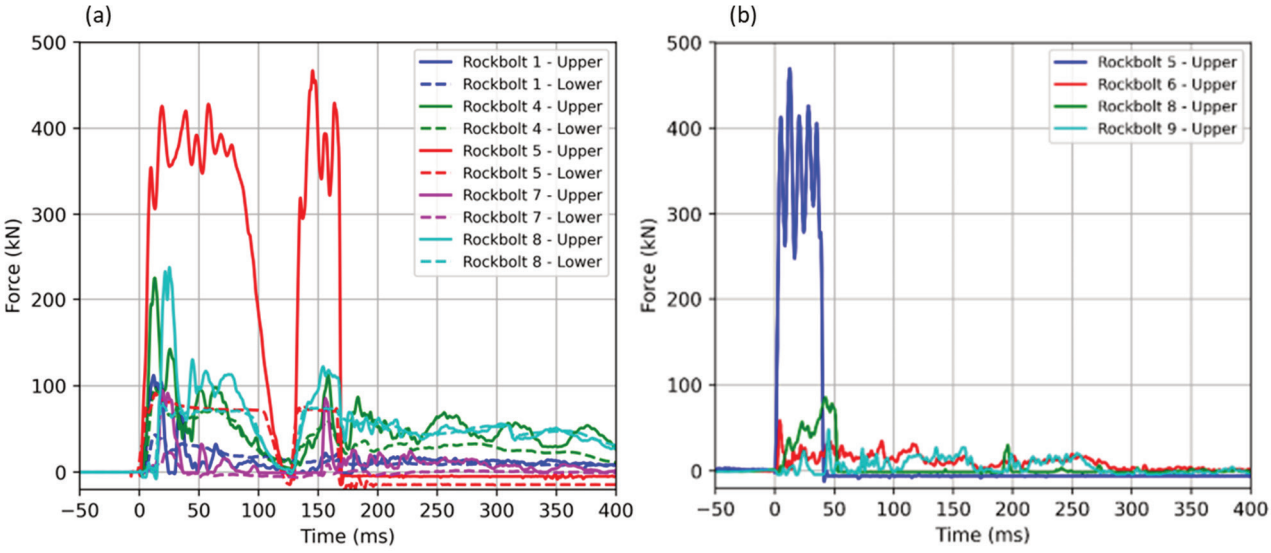

Figure 12 **(a) Test 2019: Measured load capacity on the five rockbolts by the load cells through the dynamic test as a function of time; (b) Test 2021: Measured load capacity on the four rockbolts by the load cells through the dynamic test**

Table 3 **Maximum load capacity measured by the load cells at the rockbolts**

Test	Rockbolt ID	Max. force at collar (kN)	Max. force along the anchors (kN)
Performed in 2019	1	43	112
	4	99	226
	5	91	467
	7	24	95
	8	82	238
Performed in 2021	5		470
	6		59
	8		85
	9		48

A back-analysis was performed for both tests after measuring load capacities (accelerometers and load cells) and movement (high-speed cameras). Therefore, the input load and the input energy for both tests were determined as shown in Figure 13.

It should be noted that the measured (by back-analysis) input load and energy for the test performed in 2019 were greater than the test performed in 2021. However, the input measured energy for both tests was lower than their nominal input energies (pretests), as was announced previously.

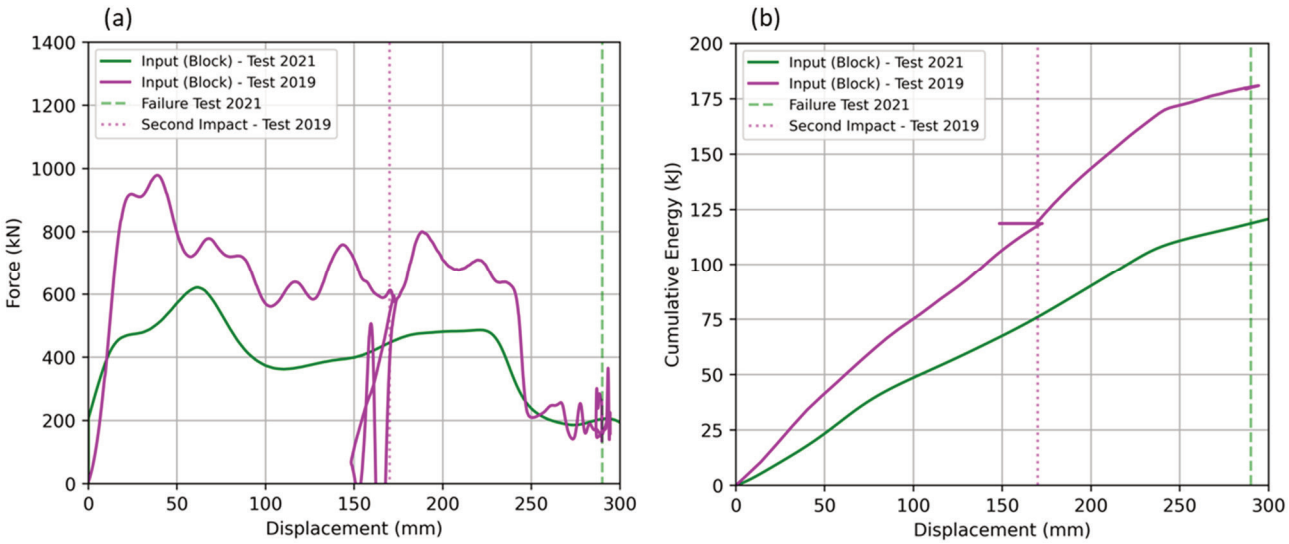

Figure 13 Back-analysis for both tests: (a) Input load; (b) Input energy

In theory, the linear energy capacity (E_c) of the ground support systems tested in 2019 and 2021 can be estimated according to Kaiser et al. (1996) and Muñoz (2019) by Equations 1 and 2, respectively. In this case, E_r is the energy absorption capacity of threadbars (A630–25 mm diameter) in a square pattern of 1 m × 1 m, $E_m^{80/4}$ is the energy absorption capacity of the chain link mesh G80/4, $E_m^{80/4.6}$ is the energy absorption capacity of the chain link mesh G80/4.6 (according to Geobrugg), and E_s is the energy absorption capacity of the shotcrete.

$$E_c^{2019} = E_r + 2 \cdot E_m^{80/4} + E_s$$
$$E_c^{2019} = 55[kJ/m^2] + 2 \cdot 12[kJ/m^2] + 1[kJ/m^2] = 80[kJ/m^2] \quad (1)$$

$$E_c^{2021} = E_r + E_m^{80/4.6} + E_s$$
$$E_c^{2021} = 55[kJ/m^2] + 18[kJ/m^2] + 1[kJ/m^2] = 74[kJ/m^2] \quad (2)$$

For the test performed in 2019, the normalised input energy of the test can be estimated dividing the maximum measured input energy of 183 kJ by the impact area (basal area of the lower loading mass: 2.56 m^2) resulting in a normalised input energy of 71 kJ/m^2. Therefore, the estimated energy capacity of the ground support system is greater than the input energy of the test measured by back-analysis. This could explain the performance of the ground support system during the test and especially the retainment system, bringing the loading masses to an equilibrium state even after the failure of the central rockbolt.

Repeating the procedure for the test performed in 2021, the normalised input energy in this case is 47 kJ/m^2 (120 kJ/2.56 m^2). Therefore, the estimated energy capacity of this ground support system is greater than the input energy of the test measured by back-analysis, which is contrary to the results. The possible explanation to this behaviour could be in the failure mode of the ground support system during the test. After the failure of the central rockbolt, the displacement of the loading mass continued, pushing the load distribution system (especially the mesh) against the external rockbolts (boundary condition), followed by the external plates cutting the mesh causing the failure of the ground support system.

From these results it is reasonable to conclude that the ground support system tested in 2019 could absorb more energy to fail completely. Whereas the ground support system tested in 2021 could have absorbed more energy if the failure mode had not been influenced by the plates. However, in order to enhance our understanding of the energy transfer process and the dynamic response of the support system, further developments are being undertaken at the at Walenstadt testing facility.

4 Conclusion

Laboratory-scale dynamic tests contribute to the knowledge, standardisation, and certification of different configurations of ground support systems. The test arrangements on these occasions allowed to study under laboratory-scale conditions the damage process in a recreated seismic event where the ground support systems are commonly used.

The results of the test performed quantified the potential energy absorption capacity of the ground support system(s) tested under dynamic loads. In the case of the test performed in 2019, the ground support system (reinforcement plus load distribution system) could absorb the total input energy without completely failing in the process. The reinforcement system mainly absorbed the energy until the first impact, where rockbolt 5 (central rockbolt) absorbed the maximum amount of energy, deforming and failing in the process. The load distribution system begins to work mainly after the second impact, bringing the loading masses to an equilibrium state and deforming in the process. In this sense, the input energy was not enough to cause the failure of the complete ground support system, being in accordance with the theoretical energy capacity of the system.

For the test performed in 2021, the ground support system could absorb the total input energy until the point of failure. The reinforcement system mainly absorbed the energy through rockbolt 5 (central rockbolt), deforming and failing in the process. The load distribution system begins to work mainly after the failure of the central rockbolt, however the boundary condition given by the external rockbolts led to the cut of the mesh and the failure of the ground support system. Compared to the previous test, there was a disagreement when the input energy and the theoretical energy capacity of the system were compared, possibly explained by the failure mode.

The measurement system was integrated with the appropriate tools to measure the load capacity, displacement and absorbed energy in the processes. A preliminary analysis of the observed behaviour and response of the dynamic loading process was presented. However, a more detailed analysis is under development to obtain an enhanced understanding of each element and the ground support systems.

These tests revealed that the current dynamic test facility at Walenstadt is an invaluable tool to test, standardise, certify, enhance, and contribute to the understanding of the behaviour of ground support systems under laboratory-scale dynamic loading. This knowledge also contributes to control seismic events and rockburst phenomenon in excavations under high stress conditions.

Acknowledgement

The authors sincerely appreciate the permission given by CODELCO – El Teniente mine to publish this paper. Also, the authors acknowledge the support from Geobrugg to collaborate with the dynamic testing facility at Walenstadt to perform the tests and actively participate during the analysis and elaboration of this document. Finally, the authors acknowledge the support from the basal CONICYT Project AFB180004 of the Advanced Mining Technology Center (AMTC) – University of Chile. The opinions expressed in this paper are those of the authors and do not necessarily represent the views of any other individual or organisation.

References

Brändle, R, Luis Fonseca, R, von Rickenbach, G, Fischer, G, Vallejos, J, Marambio, E, Burgos, L & Cuello, D 2021, 'Single impact dynamic test of a ground support system with a high-tensile steel wire mesh at the Walenstadt testing facility', *Proceedings of the Tenth International Conference on Rockburst and Seimicity in Mines*, *RaSim10,* Arizona, United States of America.

Brändle, R, Luis Fonseca, R, von Rickenbach, G, Fischer, G, Vallejos, J, Marambio, E, Burgos, L, Rojas, E, Landeros, P, Muñoz, A, Celis, S & Castro, D 2020, 'Double impact dynamic test of a ground support system at the Walenstadt testing facility', *Proceedings of the Eighth International Conference & Exhibition on Mass Mining*, *MassMin 2020,* Santiago, Chile.

Brandle, R & Luis Fonseca, R 2019, 'Dynamic testing of surface support systems', in J Hadjigeorgiou & M Hudyma (eds), *Ground Support 2019: Proceedings of the Ninth International Symposium on Ground Support in Mining and Underground Construction*, Australian Centre for Geomechanics, Perth, pp. 243-250, https://doi.org/10.36487/ACG_rep/1925_15_Brandle

Brändle, R, Rorem, E, Luis Fonseca, R & Fischer, G 2017, 'Full-scale dynamic tests of a ground support system using high-tensile strength chain-link mesh in El Teniente mine, Chile', *Proceedings of the First International Conference on Underground Mining Technology*, Australian Centre for Geomechanics, Perth, pp. 25–43.

Bucher, R, Cala, M, Zimmermann, A, Balg, C & Roth, A 2013, 'Large scale field tests of high-tensile steel wire mesh in combination with dynamic rockbolts subjected to rockburst loading', *Proceedings of the Seventh International Symposium on Ground Support in Mining and Underground Construction,* Australian Centre for Geomechanics, Perth.

Cai, M & Kaiser, PK 2018, *Rockburst Support Reference Book. Volume I: Rockburst phenomenon and support characteristics*, MIRARCO – Mining Innovation, Laurentian University, Sudbury, Ontario, Canada.

Cala, M, Roth, A & Roduner, A 2013, 'Large scale field tests of rock bolts and high-tensile steel wire mesh subjected to dynamic loading', *ISRM International Symposium-EUROCK 2013*, International Society for Rock Mechanics and Rock Engineering.

Crompton, B, Berghorst, A & Knox, G 2018, *A new dynamic test facility for support tendons*, New Concept Mining.

Hadjigeorgiou, J & Potvin, Y 2011, 'A critical assessment of dynamic rock reinforcement and support testing facilities', *Rock Mechanics and Rock Engineering*, vol. 44, pp. 565–578.

Kaiser, PK, McCreath, DR & Tannant, DD 1996, *Canadian rockburst support handbook*, Geomechanics Research Centre, Laurentian University, Sudbury, 314 p.

Muñoz, A 2019, 'Ground support systems at CODELCO, El Teniente mine', Internal Report.

Muñoz, A, Brändle, R, Luis Fonseca, R & Fischer, G 2017, 'Full-scale dynamic tests of a ground support system using high-tensile strength chain-link mesh in El Teniente mine', *Proceedings of Ninth Symposium on Rockbursts and Seismicity in Mines RaSiM9*, Editec SA, Santiago, Chile.

Ortlepp, WD 2001, 'Performance testing of dynamic stope support test facility at Savuka', SIMRAC Report, GAP 611.

Ortlepp, WD & Stacey, TR 1998, 'Performance of tunnel support under large deformation static and dynamic loading', *Tunnelling and Underground Space Technology*, vol. 13, pp. 15–21.

Ortlepp, WD & Stacey, TR 1997, 'Testing of tunnel support: dynamic load testing of rock support containment systems', SIMRAC GAP Project, 221 p.

Player, JR, Villaescusa, E & Thompson, AG 2004, 'Dynamic testing of rock reinforcement using the momentum transfer concept', *Proceeding of the 5th International Symposium on Ground Support*, E Villaescusa & Y Potvin (eds), Perth.

Roth, A, Cala, M, Brändle, R & Rorem, E 2014, 'Analysis and numerical modelling of dynamic ground support based on instrumented full-scale tests', *Proceedings of the Seventh International Conference on Deep and High Stress Mining*, Australian Centre for Geomechanics, Perth, pp. 151–163.

Zhou, Y & Zhao, J 2011, *Advances in rock dynamics and applications*, CRC Press.